Vol 10 No 7, July 2001
1009-1963/2001/10(07)/0662-04

Chinese Physics

© 2001 Chin. Phys. Soc.
and IOP Publishing Ltd

GAMMA-RAY LIGHT CURVE AND PHASE-RESOLVED SPECTRA FROM GEMINGA PULSAR*

Zhang Li(张 力), Bian Xia(边 霞), and Mei Dong-cheng(梅冬成)†
Department of Physics, Yunnan University, Kunming 650031, *China*

(Received 1 January 2001)

We calculate the light curve and phase-resolved spectra of Geminga in a three-dimensional pulsar magnetosphere model. The light curve of gamma-rays is consistent with that observed if the magnetic inclination and viewing angle are $\sim 50^\circ$ and $\sim 86^\circ$ respectively. We also model the phase-resolved spectra of the Geminga pulsar.

Keywords: Geminga pulsar, γ-ray light curve, phase-resolved spectra
PACC: 9760G, 5170, 6180C

I. INTRODUCTION

Geminga (PSR J0633+1746) is a pulsar with a period of 237 ms and a period derivative of $\sim 1.1 \times 10^{-14}$ s^{-1}. Its period was first determined by using ROSAT[1] and EGRET observations.[2] Using the measured period and period derivative, Geminga has a characteristic age of $\sim 3.4 \times 10^5$ year and its spin-down power is $\sim 3.3 \times 10^{27}$ J·s^{-1}. The observed pulse profile by EGRET[3] has a double peak-shape with a phase separation of 0.49 ± 0.05. Furthermore, the observed phase-resolved spectra in eight parts of phase have been obtained.[3] These eight parts are: leading wing 1 (LW1), peak 1 (P1), trailing wing 1 (TW1), bridge, leading wing 2 (LW2), peak 2 (P2), trailing wing 2 (TW2) and offpulse (OP). The phase intervals of all these parts are 0.11, 0.09, 0.11, 0.15, 0.13, 0.13, 0.08 and 0.21, respectively. Theoretically, there are two kinds of γ-ray pulsar models: polar cap models[4] and outer gap models.[5] Here we will use our outer gap model[6] to explain the γ-ray light curve and the phase-resolved spectra from the Geminga pulsar.

II. MODEL

We have proposed a self-sustained outer gap model of γ-ray emission from rotation-powered pulsars.[6] In this model, the fractional height of the outer gap (f_0) in ($\boldsymbol{\Omega}$, μ) plane is limited by the pair production between the thermal x-rays with energy $E_{\rm X}(f_0)$ from the stellar surface and the γ-ray photons with energy $E_\gamma(f_0)$ emitted by the primary electrons/positrons accelerated in the outer gap, and is given by

$$f_0 \approx 5.5\ P^{26/21} B_{12}^{-4/7} \xi^{-1/7}, \tag{1}$$

where $f_0 = h_0/R_L$, h_0 is the average vertical extension (perpendicular to the magnetic field) of the outer gap, $\xi = \Delta\Phi/2\pi$ is the azimuthal width of the three-dimensional (3D) outer gap, $\Delta\Phi$ is the transverse extension of the outer gap. In the 3D case, h_0 is the average separation between two equipotential surfaces which define the boundary of the outer gap. Inside a thick outer gap, the local electric field along the magnetic field lines is approximated as $E_{||} \approx f_0^2 (r/R_L)^{1/2} B(r)$ and the local number density of accelerated particles is $n(r) = \boldsymbol{\Omega} \cdot \boldsymbol{B}/2\pi ec$. Therefore, the primary $e^\pm$ pairs in the steady state have a power-law distribution with a spectral index 16/3, because the Lorentz factor of the accelerated particles is $\gamma_e \propto (r/R_L)^{-3/8}$.[6] These accelerated particles emit high-energy γ-rays through curvature radiation inside the outer gap. The curvature spectrum for a single electron is

$$F_{\rm cur}(E_\gamma) = \frac{\sqrt{3}e^2}{h\ s} \frac{\gamma}{E_\gamma} F(y), \tag{2}$$

where E_γ is the photon energy, e is the electron charge, h is the Planck constant, s is the radius of curvature, $F(y) = \int_y^\infty K_{5/3}(z){\rm d}z$, with $y = E_\gamma/E_{\rm cur}$ and $K_{5/3}$ is the modified Bessel function of the order of 5/3. The γ-rays are produced by the primary accelerated particles through curvature radiation, which depends sensitively on the local curvature. Assuming that $x = s/R_L \approx (r/R_L)^{1/2}$, then the distribution of

*Project supported by the National Natural Science Foundation of China (Grant No. 10073008)
†Corresponding author.

the accelerated particles at radius $r_{\rm c}$ satisfies[6]

$$\frac{{\rm d}N_e}{{\rm d}x} = N_0 x^{9/4}\delta(x - x_c). \tag{3}$$

Therefore, the curvature spectrum for the accelerated particles with a power-law distribution at radius $r_{\rm c}$ is

$$F_{\rm cur}(E_\gamma, x_{\rm c}) = F_0 x_{\rm c}^{-5/3} E_\gamma^{-5/3} F(y_{\rm c}), \tag{4}$$

where F_0 is a constant and $y_{\rm c} = E_\gamma/E_{\rm cur}(r_{\rm c})$. From Eq.(4), we can calculate the γ-ray spectrum at any radial distance of the outer gap.

Now we consider the 3D structure of the outer gap. In the ($\boldsymbol{\Omega}$, μ) plane, $E_\gamma \propto r^{-13/8}$. Such a strong dependence of E_γ on r will make the cross section for pair production decrease rapidly. Since pair production must take place at the beginning of the outer gap (otherwise there will be no current passing through the outer gap), we argue that the radial extension of the outer gap must be

$$r_{\rm lim} \approx f_0 R_L. \tag{5}$$

In other words, the radial range of the pair production region is limited to a certain part ($r_{\rm lim} - r_{\rm in}$) of the entire outer gap region, where $r_{\rm in}$ is the distance of the null surface which is a function of ϕ. Since $r_{\rm lim} - r_{\rm in}(\phi) \geq 0$, it gives the extension of the outer gap along the azimuthal direction, $\Delta\phi \sim 150^\circ$ for the Geminga pulsar. Therefore, for the structure of the thick outer gap in the open field line volume of the pulsar magnetosphere, the gap height is determined by f_0. The azimuthal extension of the outer gap is $\sim 150^\circ$ and the extension along the magnetic field is from $r_{\rm in}$ to R_L. However, both outgoing and incoming $e^\pm$ flows along the magnetic field lines occur in the region $r_{\rm lim} - r_{\rm in}$ and only outgoing flow in region $R_L - r_{\rm lim}$, where $r_{\rm in}$ is the radius of inner boundary of the outer gap. Also, $r_{\rm in}$ is estimated by $\boldsymbol{\Omega}\cdot\boldsymbol{B} = 0$, and we have $r_{\rm in} \approx (4/9)R_L/\tan^2\alpha$, if the inclination angle α is large.

After determining the 3D structure of the outer gap, we can show the high-energy photon morphology inside an outer gap following our recent work.[7] In this work, a rotating dipole magnetic field structure of a neutron star was simulated. For a given magnetic inclination, the polar cap shape defines the boundary of the open volume of the magnetosphere at the stellar surface. Because the outer gap is within the open volume, we divide the open volume into many parts, in which the shape of each part at the stellar surface is the same as the polar cap shape but the size is smaller. Firstly, we determine the coordinate values (x_0, y_0, z_0) of the last closed field lines at the stellar surface. Then the coordinate values (x_0', y_0', z_0') for different parts can be determined by using $x_0' = a_1 x_0$, $y_0' = a_1 y_0$ and $z_0' = (1 - (x_0'^2 + y_0'^2))^{1/2}$ and by changing a_1. Once the polar cap shape is defined, we find the last closed field lines using the Runge–Kutta integration: (i) give a set of initial values at the stellar surface; (ii) use the Runge–Kutta integration to follow a particular field line in space and determine whether this line closes inside the light cylinder or crosses it; and (iii) iterate on the initial value until the field line is just tangential to the light cylinder. Furthermore, we assume that relativistic charged particles in the open zone radiate in their direction of propagation, i.e. along the magnetic field lines in the co-rotating frame.

For each location within the open zone, the direction of emission expressed as (ζ, Φ) is calculated, where ζ is the polar angle from the rotation axis and Φ is the phase of rotation of the star. In these calculations, the effects of travel time and aberration are taken into account. A photon with velocity $\boldsymbol{u} = (u_x, u_y, u_z)$ along a magnetic field line with a relativistic addition of velocity along the azimuthal angle gives an aberrated emission direction $\boldsymbol{u}' = (u_x', u_y', u_z')$. The travel time gives a change of the phase of the rotation of the star. Combining these two effects, and choosing $\Phi = 0$ for radiation in the (x, z) plane from the centre of the star, ζ and Φ are given by

$$\begin{aligned} \cos\zeta =& u_z', \\ \Phi =& -\phi_{u'} - \boldsymbol{r}\cdot\hat{u}', \end{aligned} \tag{6}$$

where $\phi_{u'}$ is the azimuthal angle of $\hat{u}'$ and $\boldsymbol{r}$ is the emitting location in units of R_L. We project photon emissions onto the (ζ, Φ) plane and observe the emission patterns on the sky. In (ζ, Φ) plane, the null surface can be determined easily because it consists of points at which magnetic field lines are perpendicular to the rotation axis. For a field line, the null charge crossing is the location at which the projected line crosses the equatorial line ($\zeta = 90^\circ$).

Ⅲ. DISCUSSION AND CONCLUSION

For the Geminga pulsar, $f_0 \sim 0.7$, so the $r_{\rm lim} \sim 0.7R_L$ and $\Delta\Phi \sim 150^\circ$. The reasonable value of the magnetic inclination angle is $\sim 50^\circ$. Then assuming a uniform emissivity of γ-rays, we solve the emission pattern. In the top panel of Fig.1, the γ-ray emission from a single outer gap in the (ζ, Φ) plane is shown.

Due to the azimuthal and radial limits of the outer gap by photon–photon pair production, the γ-rays emitted outwards (solid curves) from the outer gap are mainly above $\xi = 90°$ in the $(\zeta,\ \Phi)$ plane, but the γ-rays emitted inwards (dotted curves) are mainly below $\xi = 90°$ (note that the inward γ-rays are emitted in the range $(r_{\rm lim} - r_{\rm in})$ of the outer gap). We also show the polar caps and the Earth line of sight (dashed line) in the top part of the figure. In the middle part of the figure, the variation of radial distance with the pulse phase for different a_1 surfaces is shown. The pulse profile of γ-rays (histogram) corresponding to the emission pattern of the top part of Fig.1 is shown in the lower part of Fig.1. From this figure, it seems that the pulse profile of γ-rays from the Geminga pulsar can be explained in our model.

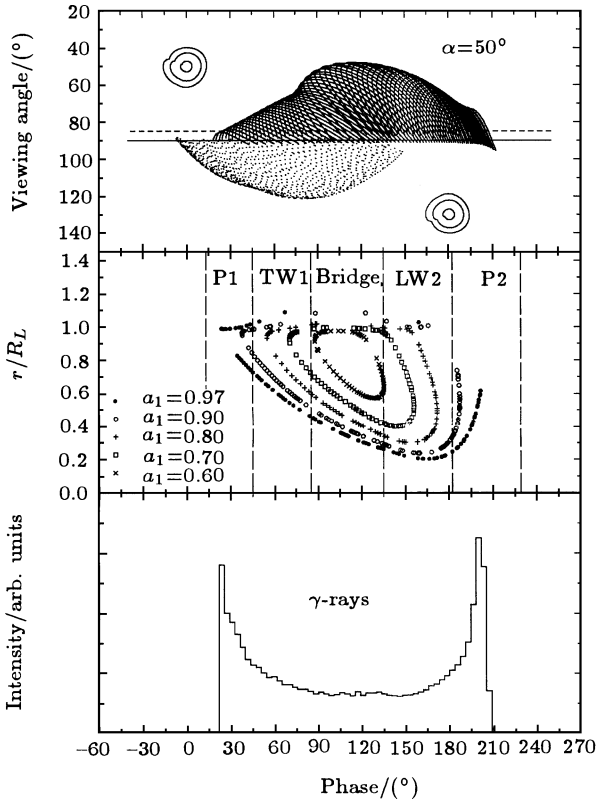


Fig.1. Emission projection onto the (ζ,Φ) plane and pulse profile for the Geminga parameter ($\alpha = 50°$). Top: photon emission from the pulsar as a function of phase, where the solid and dashed curves indicate inward and outward photon emission from a single outer gap respectively. The observed lines of sight at $\zeta = 86°$ and $\zeta = 90°$ are shown (dashed and solid lines), and both polar caps (contours) are also shown. Middle: the variation of radial distance with the pulse phase for different a_1 surfaces. Bottom: pulse profile for Geminga. The model γ-ray pulse at $\zeta = 86°$ is shown.

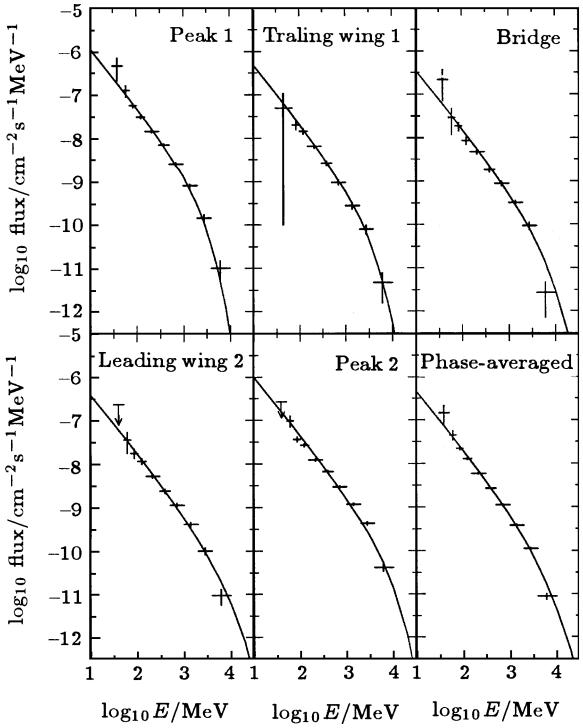


Fig.2. Phase-resolved and phase-averaged γ-ray spectra of the Geminga pulsar: peak 1, trailing wing 1, bridge, leading wing 2, peak 2 and phase-averaged. Observed data are taken from Ref.[3].

From the emission morphology we see that photons emitted into a given phase come from different positions of the outer gap. For a thick outer gap, the high-energy emission inside the outer gap can occupy a finite thickness. Since we have assumed that high-energy photons are emitted tangentially to the local magnetic field, if the viewing angle to the Geminga pulsar is known, for a single a_1 surface, the emission regions are functions of ϕ and r on the a_1 surface. Once the radial distances are determined, the spectrum of photon emission can be calculated for a given radial distance r. In order to compare with the observed phase-resolved spectra of the Geminga pulsar, we calculate the radial distances in the emission region from $a_1 = 0.6$ to $a_1 = 0.98$ for the viewing angle of 86°, and then divide the calculated pulse phases into different parts according to the division given for the observed phases.[3] Therefore, using the possible values of the radial distances for each part of the phase and Eq.(4), we calculate the phase-resolved spectra for the phases labelled peak 1, trailing wing 1, bridge, leading wing 2 and peak 2. We also calculate the phase-averaged spectrum of the Geminga pulsar. A comparison of the expected results with the observed data is shown in Fig.2. It can be seen that results based on our model are well consistent with the ob-

served data, although the components have been individually normalized. Peaks 1 and 2 are weak by factors of three and two, respectively. It should be pointed out that we have used a constant gap height in our calculations. In fact, the gap height may be variable, as pointed out by Ref.[8].

ACKNOWLEDGMENTS

We thank P L Nolan for providing us with the observed gamma-ray data of the Geminga pulsar.

References

[1] Halpern J P and Holt S S 1992 *Nature* **357** 222
[2] Bertsch D L *et al* 1992 *Nature* **357** 306
[3] Fierro J M, Michelson M, Nolan P L and Thomson D J 1998 *APJ* **494** 734
[4] Harding A K 1981 *APJ* **245** 267
Daugherty J K and Harding A K 1996 *APJ* **458** 278
Dermer C D and Sturner S J 1994 *APJ* **420** L75
[5] Cheng K S, Ho C and Ruderman M A 1986 *APJ* **300** 500
Cheng K S, Ho C and Ruderman M A 1986 *APJ* **300** 522
Chiang J and Romani R W 1994 *APJ* **436** 754
Romani R W and Yadigaroglu I A 1995 *APJ* **438** 314
[6] Zhang L and Cheng K S 1997 *APJ* **487** 370
Zhang L and Cheng K S 1998 *MNRAS* **294** 177
[7] Cheng K S, Ruderman M and Zhang L 2000 *APJ* **537** 964
Zhang L, Cheng K S and Mei D C 2000 *Chin. Phy. Lett.* **17** 544
[8] Romani R W 1996 *APJ* **470** 469